Journal of Nuclear Materials 400 (2010) 138–150

Contents lists available at ScienceDirect

Journal of Nuclear Materials

journal homepage: www.elsevier.com/locate/jnucmat

Degradation and oxidation of B_4C control rod segments at high temperatures

M. Steinbrück *

Karlsruhe Institute of Technology, Institute for Materials Research I, Postfach 3640, D-76021 Karlsruhe, Germany

ARTICLE INFO

Article history:
Received 29 October 2008
Accepted 23 February 2010

ABSTRACT

Extensive series of test were performed of the degradation of boron carbide absorber rods and the oxidation of the resultant absorber melts. Various types of control rod segments made of commercial materials used in French 1300 MW PWRs were investigated in the temperature range between 800 °C and 1700 °C in a steam atmosphere. The gaseous reaction products were analyzed quantitatively by mass spectroscopy for evaluation of the oxidation rates. Extensive post-test examinations were performed by light microscopy, scanning electron microscopy as well as EDX and Auger spectroscopy. Rapid melt formation due to eutectic interactions of stainless steel (cladding tube) and B_4C, on the one hand, and steel and Zircaloy-4 (guide tube), on the other hand, was observed at temperatures above 1250 °C. Complex multi-component, multi-phase melts were produced. ZrO_2 oxide scale on the outside kept the melt within the guide tube, thus preventing its early relocation and oxidation. Rapid oxidation of the absorber melts and remaining boron carbide pellets took place after failure of the protective oxide shell above 1450 °C. Only very little methane was produced in these tests which is of interest in fission product gas chemistry because of the production of organic iodine.

1. Introduction

Boron carbide (B_4C) is widely used as a neutron absorbing control rod material in Western Boiling Water Reactors (BWR) and Russian RBMKs and VVERs. In French Pressurized Water Reactors (PWR), it is employed in hybrid rods together with a silver/indium/cadmium alloy (SIC) [1]. In a hypothetical severe accident, B_4C reacts with the surrounding stainless steel (SS) cladding, producing eutectic melts at temperatures above 1200 °C [2–4], i.e. far below the melting temperatures of all components. After failure of the control rod (CR), both the remaining bare absorber material and the B_4C/metal mixtures are exposed to steam in the reactor core.

Oxidation of B_4C by steam is highly exothermal, producing six or seven times the hydrogen volume arising from oxidation of the same mass of Zircaloy. Furthermore, gaseous species containing carbon and boron are produced, which may affect fission product chemistry in the containment, e.g. the release of organic iodine compounds. The oxidation kinetics of pure B_4C materials has been studied extensively within the COLOSS program [5–9]. New experimental data were used as input for modeling of B_4C oxidation [10]. In the beginning of this study no data were available on the oxidation of absorber melts. Recently, the BECARRE project within the framework of the International Source Term Programme (ISTP) [11] at IRSN was initiated to study the oxidation of boron carbide-metal mixtures.

The main objective of the work presented here was to investigate the degradation and failure of B_4C-bearing control rod segments and the resultant release of gaseous species containing carbon and boron. Various types of specimens were investigated in the temperature range between 1000 °C and 1700 °C, namely control rod segments the size of one pellet of two different designs, 10 cm long control rod segments, and SS/B_4C/Zry-4 absorber melts of various compositions. Moreover, the ability of boron carbide to liquefy stainless steel far below the melting temperature was investigated in special tests.

The experimental program was run at the Karlsruhe Research Center (FZK, now Karlsruhe Institute of Technology, KIT) within the COLOSS project of the 5th Euratom Framework Program. It is closely associated with the FZK bundle tests QUENCH-07 [12] and QUENCH-09 [13] with a B_4C control rod, and the French Phebus FPT-3 test [14]. The results presented in this paper summarize experimental report FZKA-6980 [15].

2. Experimental setup, specimens, and test procedure

Three experimental setups were used for the experiments described in this paper: the BOX rig, the single-rod QUENCH-SR rig, and the LAVA furnace described in detail elsewhere [15].

All tests of small specimens the size of one pellet and the oxidation tests of absorber melts were performed in the BOX rig consisting of (1) a gas supply system for Ar, H_2, and steam (0–4 mol/h

* Tel.: +49 7247 822517.
E-mail address: martin.steinbrueck@kit.edu.

0022-3115/$ - see front matter © 2010 Elsevier B.V. All rights reserved.
doi:10.1016/j.jnucmat.2010.02.022

each), (2) a horizontal tube furnace with an alumina reaction tube with maximum operating temperatures of 1700 °C, and (3) a Balzers GAM 300 quadrupole mass spectrometer (MS) for quantitative analysis of all gaseous reaction products. In most of the tests, the hydrogen release rate was used as a continuous measure of reaction kinetics. The mass spectrometer was calibrated for H_2, CO, CO_2, and CH_4 with certified Ar-5% gas mixtures, and for steam by means of the Bronkhorst CEM (controlled evaporator mixer) system also used for steam supply in the tests. The furnace temperature was measured and controlled by two Pt/Rh thermocouples surrounded by an alumina tube closed on one side and located near the specimen in the reaction tube.

The QUENCH-SR rig was used for tests with longer control rod segments approx. 10 cm in length. The specimen is heated by an induction coil around the section of a quartz tube enclosing it. Power is supplied to the coil from a 20 kW oscillator at a frequency of 700 kHz. The temperature was controlled by a pyrometer and measured by a thermocouple attached to the surface of the control rod segment at mid-axial position.

The SS/B_4C/Zry-4 melts were prepared in the LAVA furnace in an inert atmosphere. This induction furnace with a tungsten susceptor is powered by the same HF oscillator as the QUENCH-SR rig. Its maximum operating temperature is 2300 °C. The LAVA furnace was also used for the B_4C-stainless steel dissolution tests.

Various types of specimens were investigated, as can be seen in Fig. 1. The materials under study were commercial control rod materials as used in French 1300 MW PWRs; they were supplied by Framatome. The boron carbide pellets (Framatome, diameter 14 mm, height 7.47 mm, 70% density) are surrounded by a stainless steel cladding tube (Framatome, AISI 308 modified, outer diameter 9.68 mm, inner diameter 7.72 mm) and the Zircaloy-4 guide tube (outer diameter 10.92 mm, inner diameter 10.12 mm).

The small specimens with metal plugs, and the long specimens were identical in design. They were electron beam welded under a vacuum. A zirconia disc was used to separate the B_4C pellet and SS cladding from the Zircaloy plugs. Some of the long specimens were subsequently filled with helium to show the influence of internal pressure buildup. In addition, CR segments the size of one pellet, with ceramic caps, were studied. They were characterized by the very same mass ratio, B_4C:SS:Zry-4, as the commercial absorber rod.

The SS/B_4C/Zry-4 absorber melts were prepared in the LAVA furnace. Tests with pressed powder mixtures failed. These specimens did not melt completely, or showed a large void volume probably due to the high surface areas and the generation of protective oxide scales on the grain surfaces. For this reason, thin discs of the respective materials were stacked in a shallow zirconia crucible and molten at temperatures between 1900 °C and 2100 °C.

Finally, experiments about the eutectic interaction between boron carbide and stainless steel were performed with Framatome B_4C pellets and SS (AISI 304) hollow cylinders, as illustrated in Fig. 2.

The specimens used in oxidation tests were usually were heated in an inert atmosphere (50 l/h at standard conditions, i.e., 0 °C and 1 bar in the BOX, and 100 l/h in the QUENCH-SR rig) up to 800 °C. Then, steam injection was switched on, usually at flow rates of

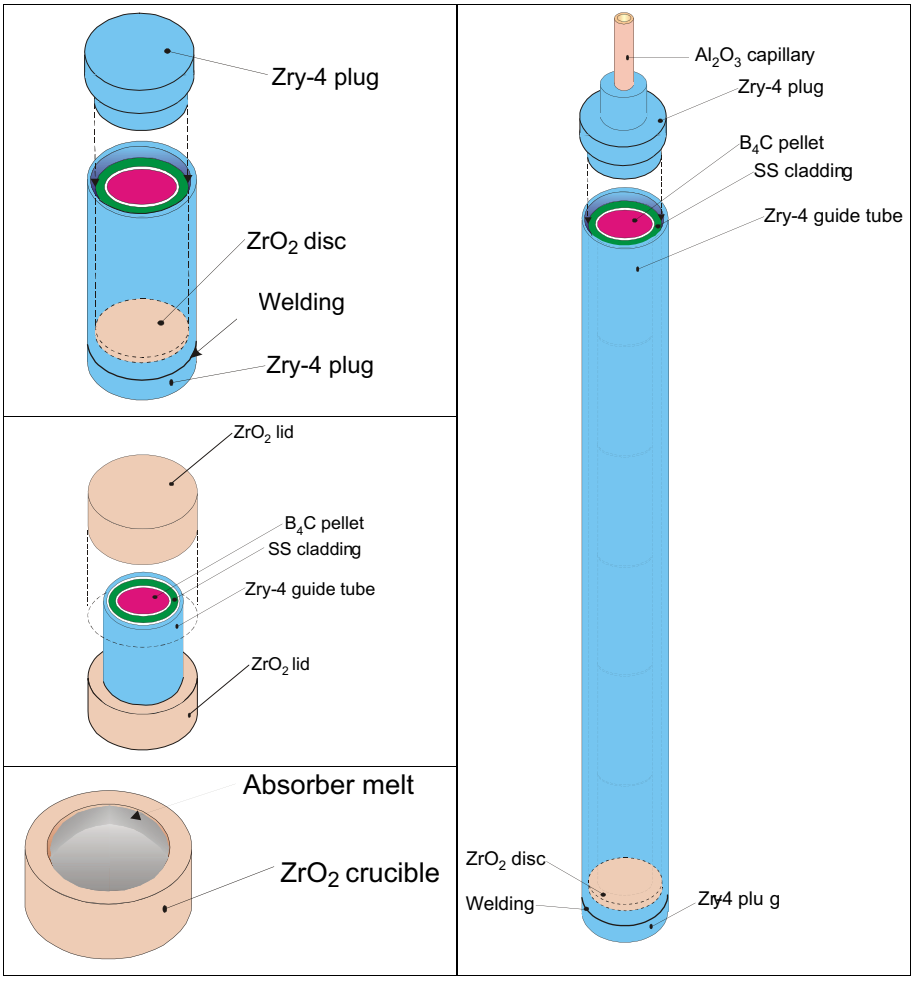

Fig. 1. Specimens used in control rod degradation and oxidation tests.

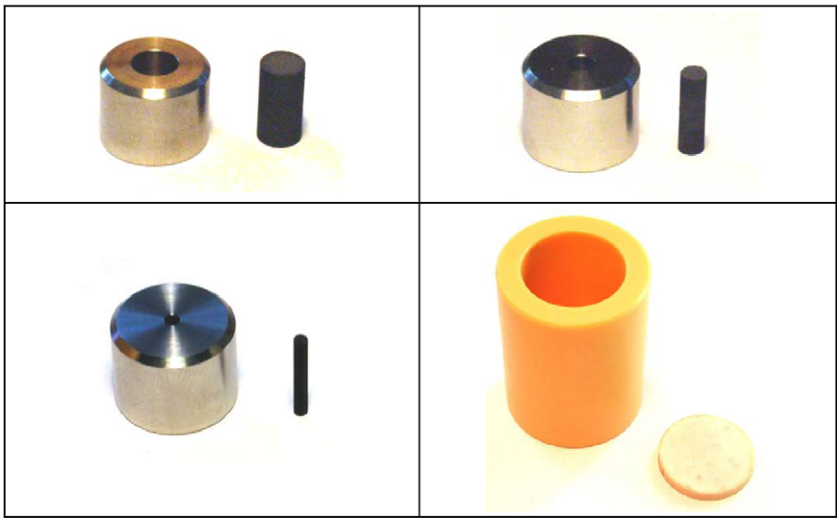

Fig. 2. Stainless steel/boron carbide specimens with large (5 wt.%), medium (1 wt.%), and small (0.3 wt.%) B_4C pellets. The frame on the lower right shows the ZrO_2 crucible and the Y_2O_3 cover plate.

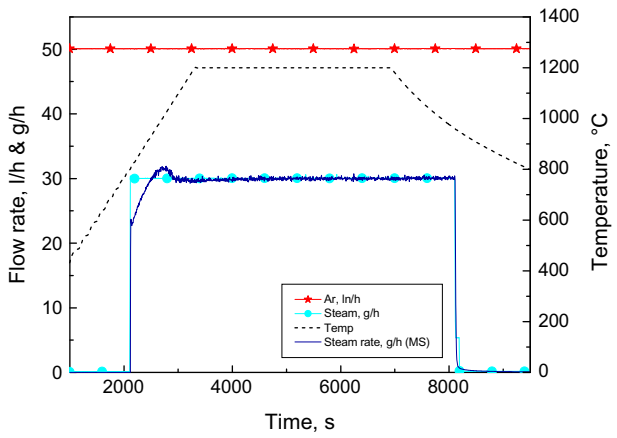

Fig. 3. Typical isothermal test, in this case, at 1200 °C.

30 g/h in the BOX and 100 g/h in the QUENCH-SR tests, and the specimens were heated to the desired temperature. Oxidizing conditions were chosen relatively early in the heating phase to prevent degradation of the specimens as seen in tests under an inert atmosphere (see Chapter 3.1). Fig. 3 shows a typical isothermal oxidation experiment in the BOX rig. The mass flow rates of the steam injected by far exceeded the amount of steam consumed by the oxidation reaction, as can be seen from the two steam curves (injected, offgas) in the diagram. Thus, no steam starvation was expected to occur in these tests. The heating rate in the heat-up phase and in the transient tests was 20 K/min. The test procedure and the results of the MS gas measurements of all tests are compiled in [15].

Experiments on the eutectic interaction between SS and B_4C were performed under inert conditions in the LAVA furnace. The specimens were heated at 1 K/s to the desired plateau temperature of 1250 °C; heating was turned off at the end of the isothermal phase.

For post-test analysis, the specimens were embedded in epoxy resin, ground and polished. Light microscopy and scanning electron microscopy (SEM) were used for metallographic examination, energy dispersive X-ray spectroscopy (EDX) and high-resolution Auger spectroscopy, for elemental analysis.

3. Experimental results

The main experimental results of the test series will be presented and discussed in the following section.

3.1. Transient tests of one-pellet-sized specimens in different atmospheres

Some initial transient tests between 800 °C and 1500 °C were performed in oxidizing and inert atmospheres to assess the behavior of the control rod segments at high temperatures. Degradation

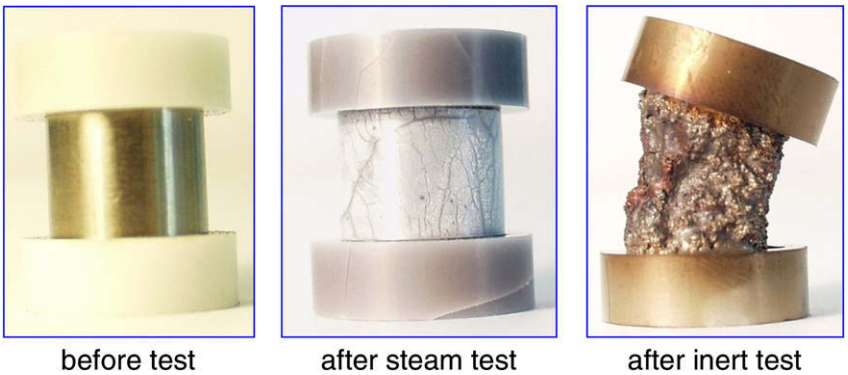

Fig. 4. B_4C control rod segments after transient tests between 800 °C and 1500 °C in oxidizing and inert atmospheres.

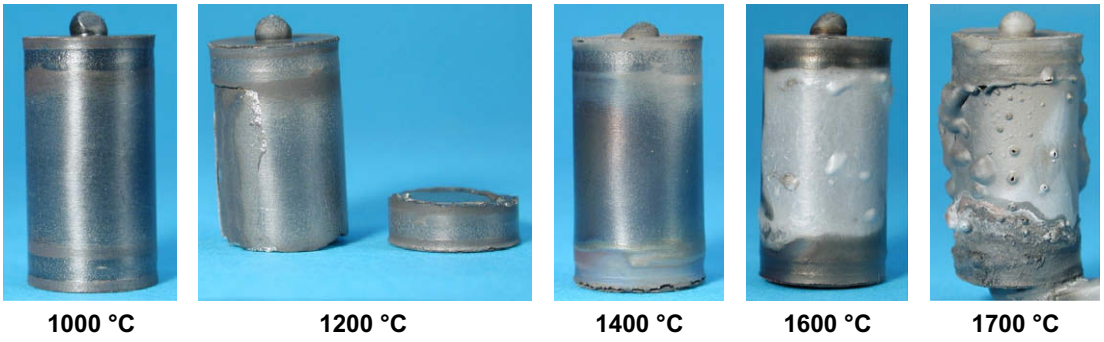

Fig. 5. Post-test appearance of the specimens after 1 h of isothermal testing at the temperatures indicated.

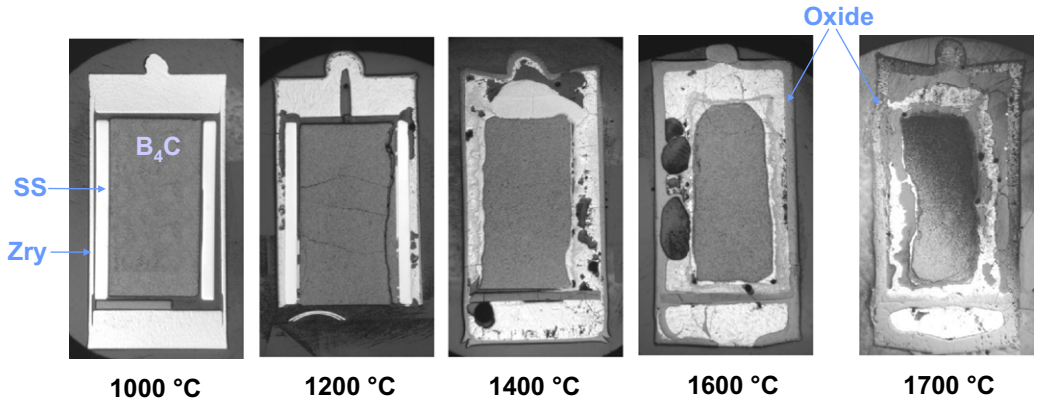

Fig. 6. Cross sections of short B_4C control rod segments after isothermal tests at the temperature indicated for 1 h.

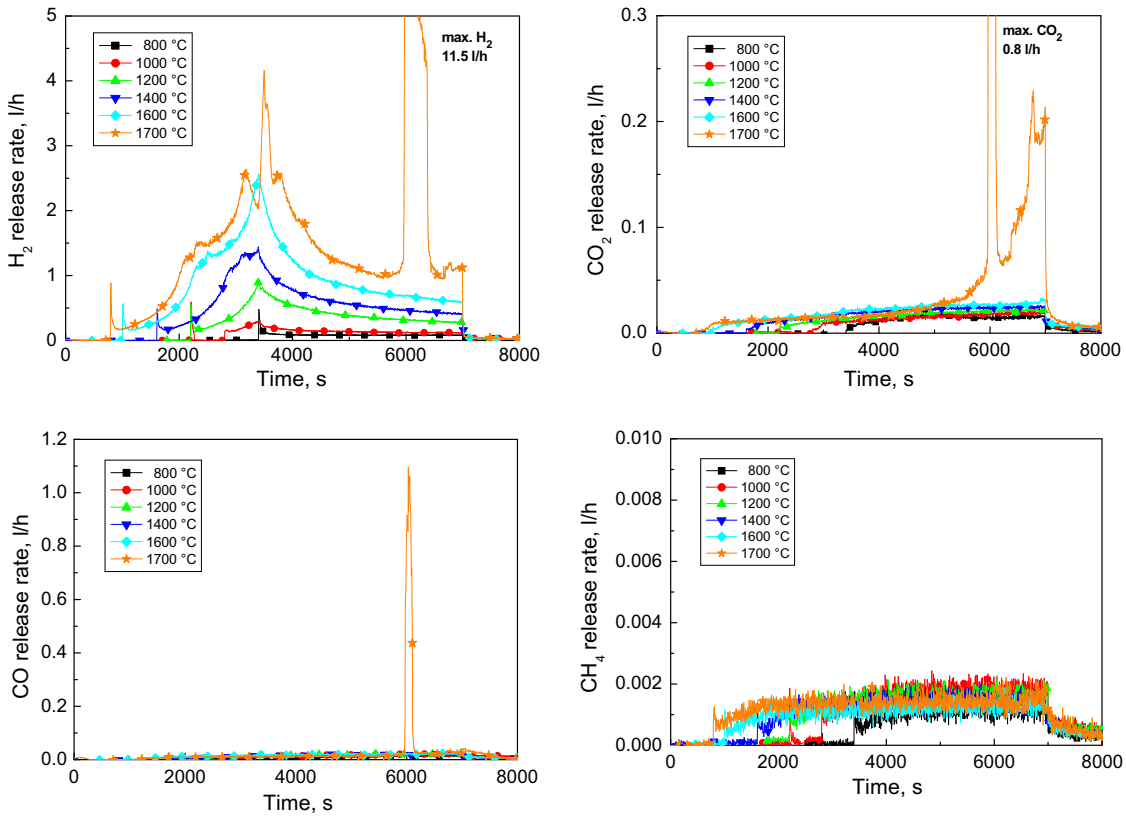

Fig. 7. Gas release in isothermal oxidation of short B_4C control rod segments with metal plugs in steam.

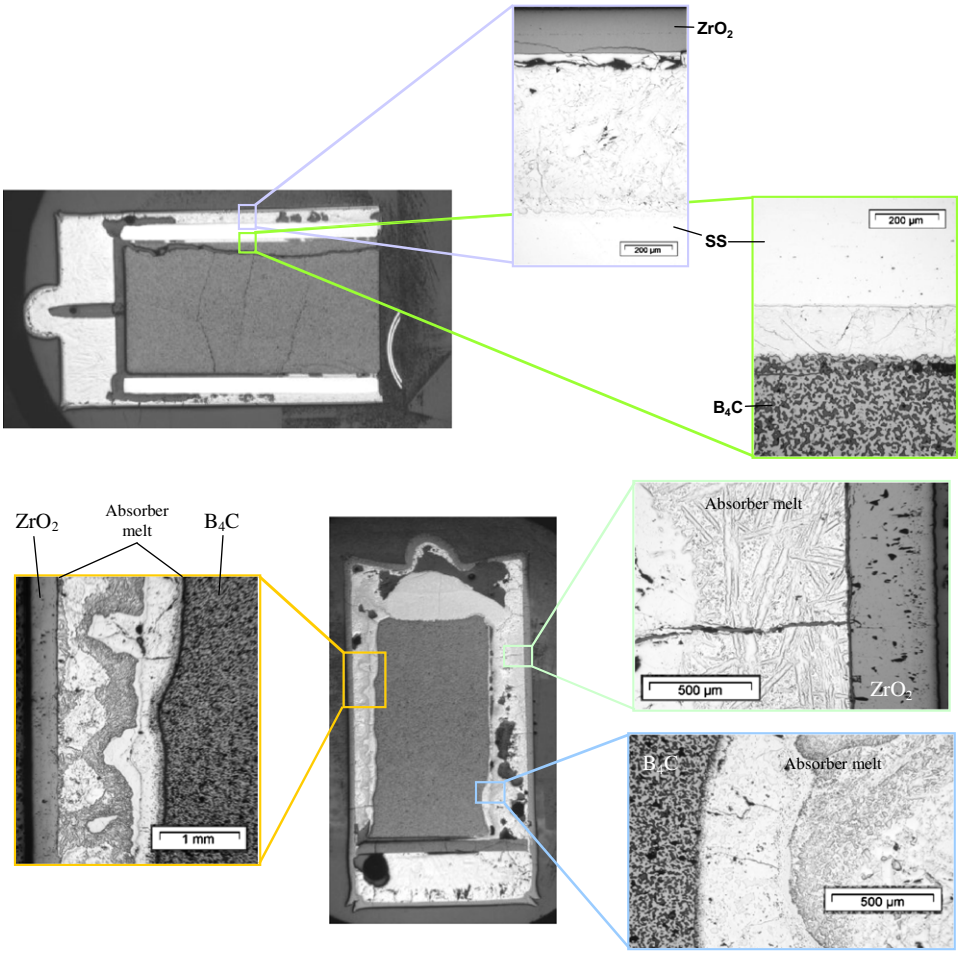

Fig. 8. Metallographic post-test examination of the CR specimens after isothermal oxidation at 1200 °C (top) and 1400 °C (bottom).

of the control rods strongly depends on the atmosphere (Fig. 4). The specimen examined in an inert gas atmosphere was degraded completely by the eutectic interactions of the stainless steel cladding and the Zircaloy guide tube as well as stainless steel and B_4C. The specimen heated in an oxidizing Ar/steam flow was prevented from failing by the formation of an outer ZrO_2 oxide scale which confined the melt and prevented its relocation.

3.2. Isothermal test series with one-pellet-size specimens with metal plugs

In an isothermal test series, specimens with metal plugs were kept in a steam/argon atmosphere at temperatures between 800 °C and 1700 °C for 1 h. Fig. 5 shows the post-test appearance of the specimens, and Fig. 6 shows axial cross sections of the samples.

No interactions at all among the components took place up to 1000 °C. Minor interactions of SS and B_4C as well as SS and Zircaloy-4 accompanied by local melt formation were observed at 1200 °C. Significant melt production was seen at temperatures of 1400 °C and above. The steel cladding was completely dissolved in these tests, consumption of the boron carbide pellet due to interaction with the metal melts increased with temperature. The ZrO_2 scale produced on the outside prevented the specimens from early failure. Only in the 1700 °C test, did the scale fail after approx. 40 min, leading to the access of steam to B_4C and absorber melt accompanied by the pronounced production of CO and CO_2 plus additional hydrogen, as can be seen in Fig. 7. As in the oxidation of pure B_4C [5], almost no methane is released in the high-temperature oxidation of absorber melt.

Extensive post-test examinations were performed by light microscopy, SEM/EDX and Auger analysis. The findings are presented in Annexes A6 and A7 of [15]. Some significant results of the work will be discussed below. Fig. 8 shows the incipient interaction of the components of the control rod with local melt production for the 1200 °C specimen. Liquid interaction layers are generated between Zircaloy and the still solid steel guide tube and between B_4C and steel. After the test at 1400 °C a complex multi-component, multi-phase mixture is enclosed in the gap between the B_4C pellet and the outer oxide scale (see also Fig. 10).

Fig. 9 shows EDX linescans through the Zry/SS/B_4C arrangement after tests at 1200 °C and 1400 °C. Both samples show two zirconium concentration peaks, one at the outer surface of the specimens with an oxide scale, and one in the gap between the stainless steel cladding and the B_4C pellet. Obviously, Zircaloy-bearing eutectic melts filled the gap due to capillary forces from the top of the specimen where Zircaloy from the plugs was available.

The most detailed phase distribution findings were obtained by Auger analysis. Fig. 10 shows a detail of the solidified melt after the test at 1400 °C. On the left-hand side of the magnified image there are boride phases of the steel components, Fe, Cr, Ni. Phases rich in Ni and Cr are separated from each other as was observed also for

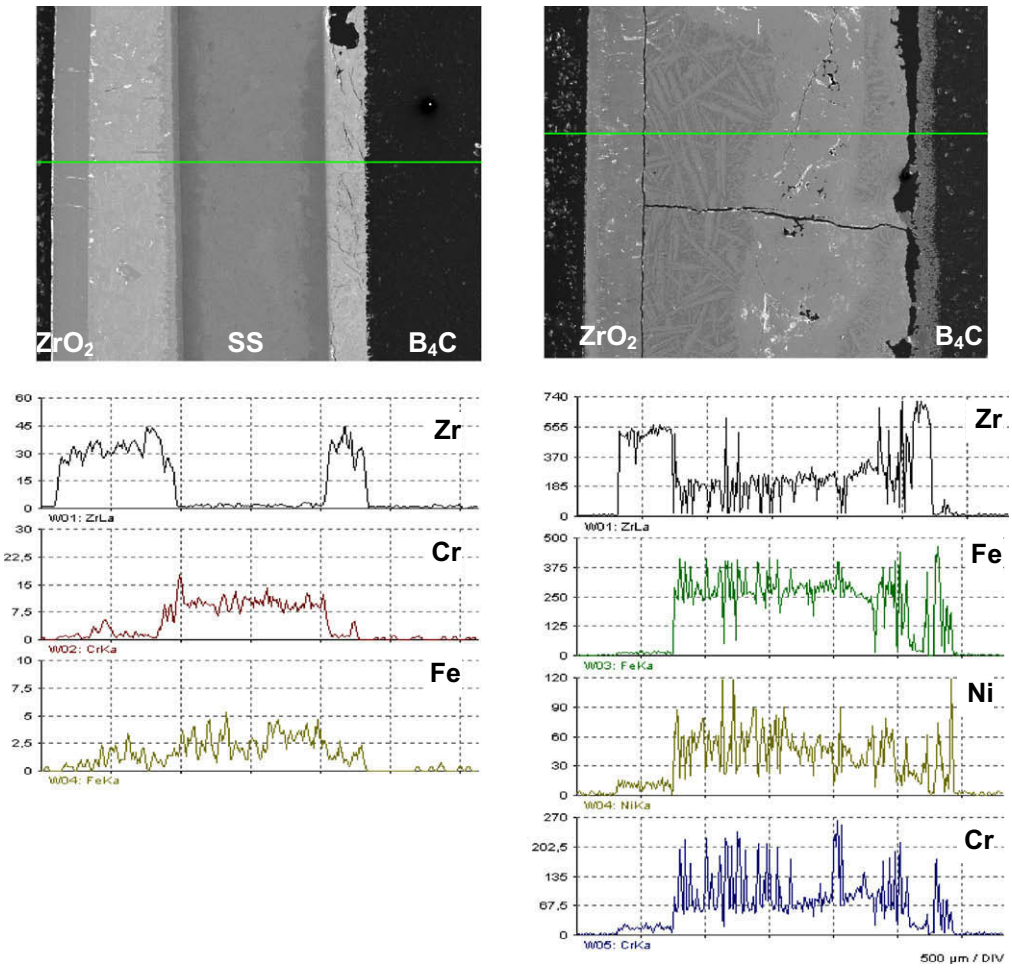

Fig. 9. EDX linescans through the sequence of layers in a control rod after isothermal tests at 1200 °C (left) and 1400 °C (right).

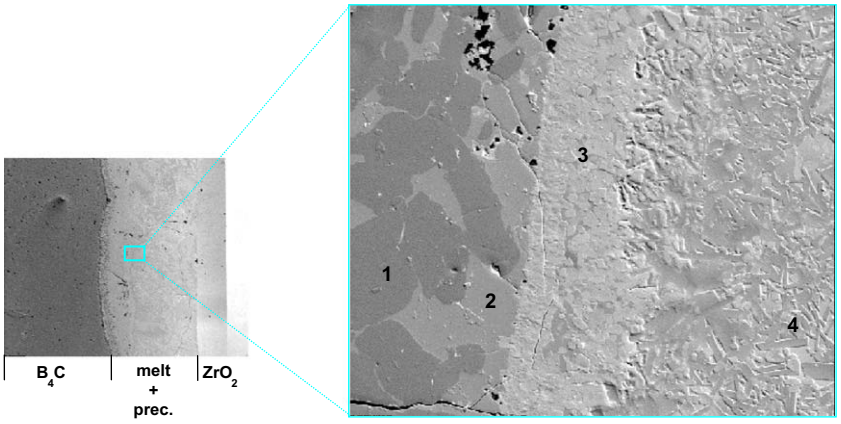

Fig. 10. Phase composition of the solidified melt in the gap between the B_4C pellet and the outer oxide scale after an isothermal test for 1 h at 1400 °C in steam. (1): (Fe, Cr) boride, (2): $(Fe, Ni, Cr)_2$ boride, (3): Zr (oxo-)carbides, (4): Zr boride in a metal matrix.

the other specimens. Phase diagrams show a miscibility gap in the solid state in the Cr–Ni system whereas Fe–Cr and Fe–Ni are completely miscible [16] (listed in [15]). The boride phases of the steel components (especially of Ni) have relatively low melting points. The melting points of zirconium boride and carbide are well above 3000 °C. It is safe to assume, therefore, that the round Zr carbide phases, which are concentrated at the boundary to the Fe, Cr, Ni borides, and the longish, sometimes needle-like Zr boride phases originated in the test at temperature. These kinds of phases were found in all specimens producing melts as can be seen from the many pictures in the Annex of [15] and in Fig. 11 in the detailed SEM images of the 1600 °C specimen.

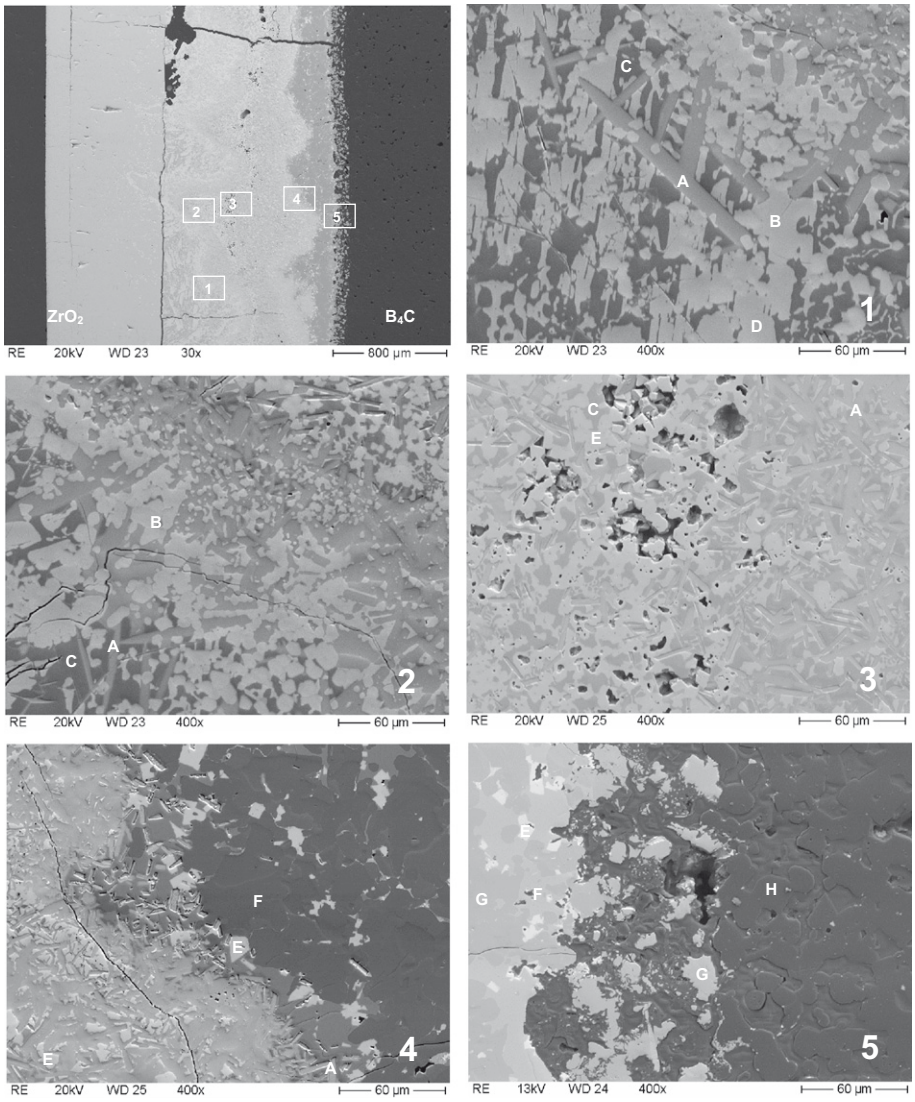

Fig. 11. SEM images of the CR specimen after isothermal oxidation for 1 h at 1600 °C illustrating the multitude and complexity of phases in the solidified melt.

3.3. Isothermal test series of one-pellet-sized specimens with ceramic caps

Another series of isothermal tests were conducted on specimens of a different design, namely with ceramic caps instead of metal plugs. These simpler specimens have the same mass ratio of the B_4C, stainless steel, and Zircaloy components as the entire rod, which is an advantage compared to the first type of samples.

Unlike in the first isothermal series, failure of the external oxide shell already occurred at 1500 °C (Fig. 12) and was accompanied by a very rapid, almost explosion-like reaction of the absorber melt and/or the remaining boron carbide pellet with steam. After the test at 1600 °C, only the oxide shell and a frozen droplet of metal were left. Huge volumes of hydrogen, CO, and CO_2 as well as boric acids were produced during that period, as can be seen in Fig. 13. No methane (CH_4) was produced in any of the tests. The melt was sprayed onto the top of the reaction tube of the BOX Rig in one test at 1500 °C. The specimen was dislocated in the alumina boat, and a large volume of condensed boric acids was found at the outlet flange of the reaction tube. The offgas pipes were blocked by the boric acids; mass spectrometric measurements thus were no longer possible after this test phases at 1600 °C.

Hydrogen release rates increased by a factor of 30 after failure due to the rapid reaction of the B_4C-bearing melt as shown in Fig. 13. Up to 40% of the initial mass of B_4C was oxidized after failure of the zirconia shell at high temperatures due to the release of all carbon monoxide and carbon dioxide. The actual levels may be even higher, as the MS measurement in the late phases of some of the tests was affected by (partial) blockage of the offgas system.

The polished cross sections of the specimens with ceramic caps (Fig. 14) look similar to the specimens with metal plugs. After 1 h at 1200 °C the components of the control rod segments interacted only slightly. No melt production was observed after this test. At 1300 °C and above the stainless steel cladding was liquefied completely in the eutectic reactions with B_4C and Zircaloy. As expected, the dissolution of B_4C by stainless steel increased with temperature.

The microscope images show many different phases which were then identified by Auger analysis. Near the B_4C pellet a (Fe, Cr)B/(Fe, Cr, Ni)$_2$B (matrix) mixture is predominant in all specimens. Also ZrC and Zr(C, O) were found in this region. These phases were observed mainly in a SS matrix near the external ZrO_2 oxide scale. A clear separation between phases containing Cr and Ni was

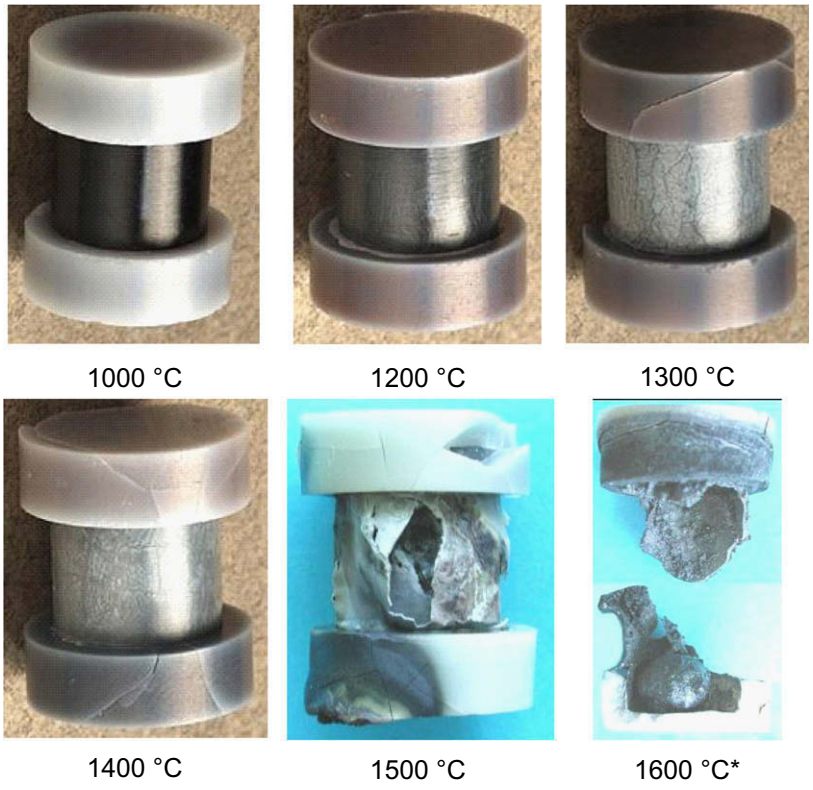

Fig. 12. Post-test appearance of the specimens with ceramic caps after 1 h of isothermal testings at the temperatures indicated in an Ar/steam flow.

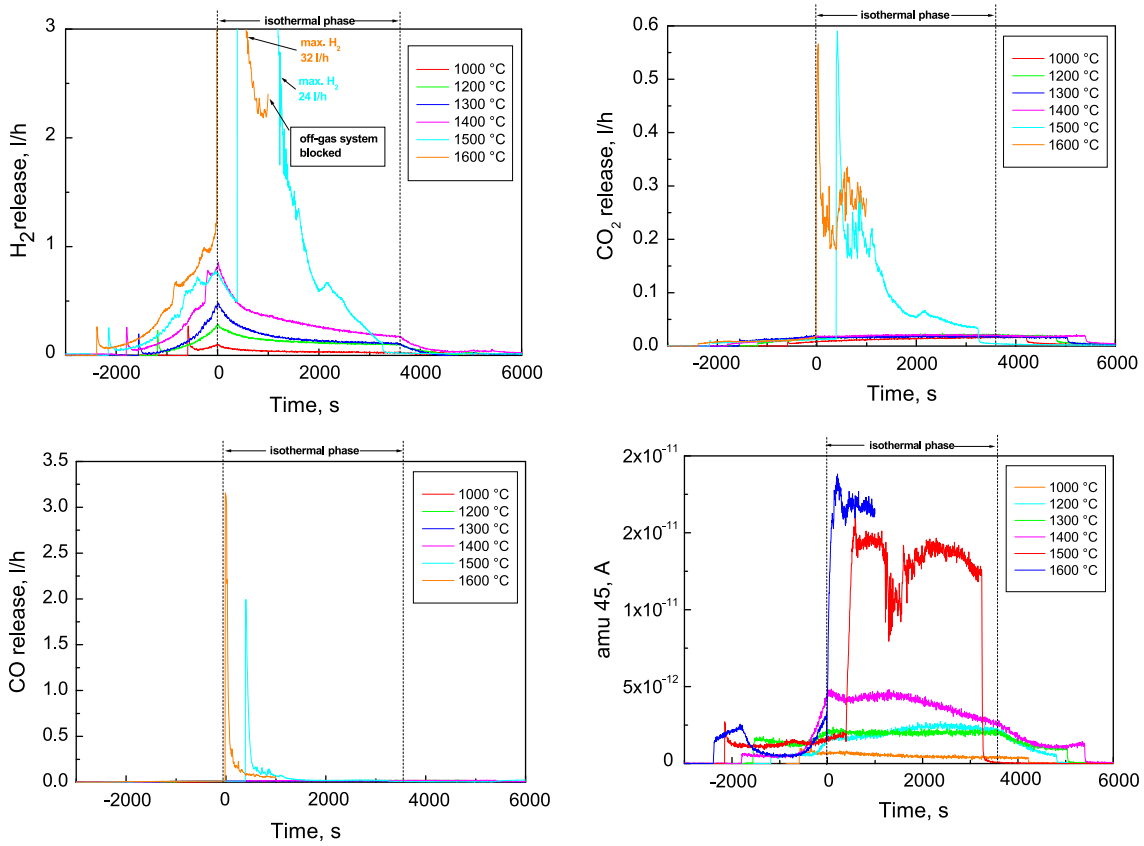

Fig. 13. Gas and boric acid releases during isothermal tests in an Ar/steam atmosphere at the temperatures indicated.

seen in all specimens. Sn enrichment was found in Ni phases. Other phases were identified as NiB, CrC_2, ZrB_2, $Zr(B, C)_x$, and $Zr(B, C, O)_x$. Diffusion of the elements and/or convection of the melt increased with rising temperature. On the one hand, the oxygen content near the B_4C pellet and, on the other hand, the boron and carbon concentrations near the ZrO_2 scale increased with temperature. Boron was found mainly in the metal phase (SS borides), while carbon occurred in the oxide phase (Zr(O ,C)). The total amount of boron in the melt increased with temperature, indicating higher dissolution. Chromium was enriched near the B_4C pellet, especially at higher temperatures.

3.4. Tests of 10 cm specimens in the QUENCH-SR rig

Fourteen tests were conducted with 10 cm long specimens induction-heated in the QUENCH-SR rig. The first three tests were performed on specimens held in position from the top by a Zircaloy capillary tube. After failure the specimens dropped and could no

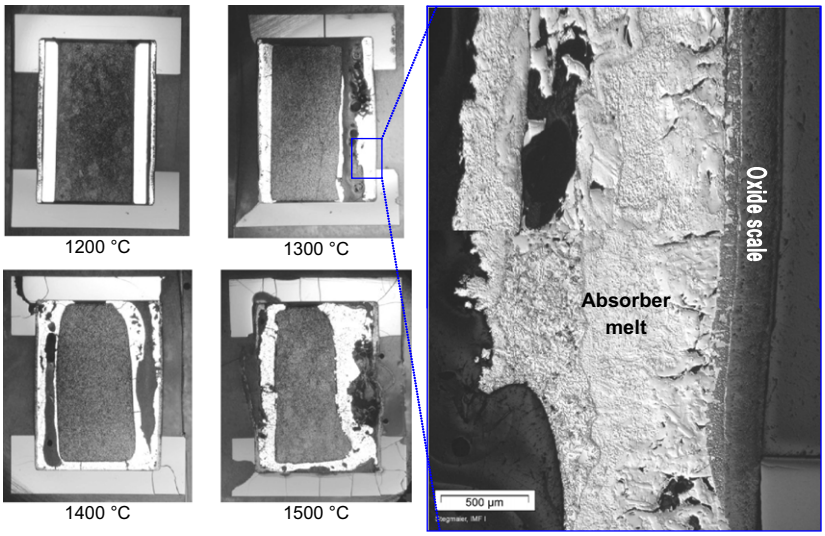

Fig. 14. Cross sections through specimens with ceramic caps after isothermal oxidation in an Ar/steam flow for 1 h at the temperatures indicated.

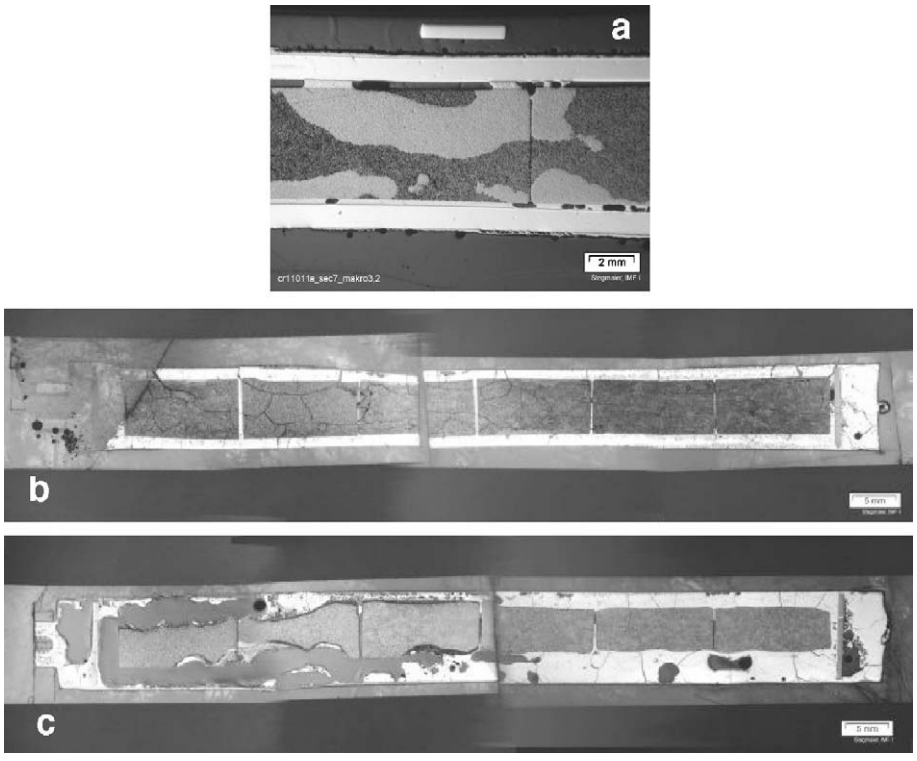

Fig. 15. Axial cross sections of the 10 cm long control rod segments: (a) after 0.1 K/s heating to approx. 1100 °C, showing local interactions of SS with B_4C; (b) after 1 K/s heating to 1430 °C, showing complete liquefaction of SS in the ZrO_2 shell; and (c) after 1 K/s heating to 1580 °C, showing strong local oxidation of B_4C pellets at the points of failure and significant dissolution of B_4C pellets.

longer be heated. A new sample support was then designed and built, which held the specimen in position even after failure and allowed further heating. Isothermal tests at 1250–1560 °C as well transient tests at heating rates of 0.1, 1, and 3 K/s were run. Two tests were conducted in an inert atmosphere, all other tests, in Ar/steam. All test parameters are summarized in [15].

The two specimens heated in an inert atmosphere show melt formation and relocation at relatively low temperatures even from the outside. The ZrO_2 oxide scale produced in the tests run in a steam flow protects the B_4C pellets and the absorber melt inside from steam as long as it is intact. Only after failure of the oxide shell (break, dissolution by absorber melt from the inside), boron carbide was oxidized locally near the position of oxide failure, as can be seen from selected axial cross sections of the specimens (Fig. 15). This was confirmed by the MS gas analyses showing significant releases of CO and CO_2 only above 1450 °C. The eutectic melt relocated downward inside the annulus between the pellet and the oxide shell. It also partly filled the gaps between the boron carbide pellets, which is indicative of the low viscosity of the melt.

The image of the specimen after a test finished at relatively low temperatures (1040 °C) clearly shows the initial local character of the interaction of the stainless steel cladding with the B_4C pellet (Fig. 15a). The stainless steel cladding melted/reacted completely in almost all other specimens. As in the tests of the one-pellet-size specimens, the solidified melt is a complex mixture of many phases not examined further here.

The failure temperature (i.e. the temperature at which significant releases of CO and CO_2 were observed) is between 1470 °C and 1580 °C, which is in agreement with the results obtained on the small specimens. No significant difference between specimens kept in a vacuum and those filled with helium was observed except for their macroscopic appearance after the test.

3.5. Oxidation of SS/B_4C/Zry-4 absorber melts

The experiments performed on prototype control rod segments indicated very high oxidation rates of the absorber-metal melts released after failure of the oxidized Zircaloy guides tube. Consequently, separate-effects tests on the oxidation of such melts have been conducted. The composition of these melts was derived from the analyses of eutectic melts produced in the control rod tests. Table 1 shows the compositions of specimens studied. Tests of pure stainless steel and Zircaloy-4 were conducted for comparison. For the same reason, a test of pure B_4C performed earlier under very similar conditions was taken into account [5].

The composition of the sample melt, especially its melting point, has a strong influence on oxidation kinetics and, thus, on gas release as shown in Fig. 16. Pure boron carbide and pure Zircaloy, which are in a solid state throughout the test, have relatively low and smooth oxidation rates. The same is true for steel up to its melting point at approx. 1410 °C. After melting, the oxidation rate rises steeply and becomes more unstable. Eutectic interaction causes the mixed absorber melts to melt at lower temperatures, which leads to significantly higher oxidation rates at lower temperatures. The first gas production peak in the test of 5% B_4C – 95% SS was measured at 1170 °C. The maximum oxidation rates of the melts are more than one order of magnitude higher than those of solid materials at the same temperatures.

Rates scatter widely as a result of the production of inhomogeneous, unstable oxide scale. This unstable behavior may be caused also by rapid local oxidation associated with spraying and fragmentation of the melt, as became apparent in some tests from the appearance of the crucibles. Small fragmented melt particles offer a large surface to the steam and are consumed very rapidly.

There is also a tendency of lower oxidation rates with increasing amounts of B_4C and Zircaloy in the steel (Fig. 16). It is assumed that the content of solid phases in the melt increases, thus causing an increase in viscosity of the mixture and impeding convection in the melt.

The CO/CO_2 ratio measured increases with increasing Zircaloy content of the mixture due to the highly reducing properties of zirconium. Methane production is negligible in all tests; a small, but measurable, CH_4 release was observed only at the onset of oxidation of pure B_4C.

Fig. 18 shows the cross sections of all melt specimens after oxidation. During preparation of the melts under inert conditions, no interactions of the melt with the zirconia crucible were observed even at temperatures above 2000 °C. However, under oxidizing conditions, the interaction of melt with the crucible is strong already at lower temperatures (800–1550 °C, 20 K/min), becoming more intense with growing complexity of the melt. Degradation of the crucible seems to be driven by the generation of zirconium oxocarbides and eutectic interactions of ZrO_2 with Fe_2O_3.

Obviously, the oxidation of the melts is not controlled by protective oxide scale forming, which is one reason for the high oxidation rates discussed above. In the pseudo-binary SS–B_4C system maximum oxidation was obtained for the sample with the lowest boron carbide content. That composition is near eutectic (e.g., the Fe–B phase diagram shows the lowest eutectic temperature for 17% B or approx. 4 wt.% B, see Fig. 17). With increasing content of B_4C in the mixture, its composition more and more differs from eutectic, the liquidus temperature rises, thus causing less oxidation. The melt with 20 wt.% B_4C thus corresponds to the composition of iron boride, FeB, in the binary phase diagram, Fe–B, with a melting point of 1650 °C. The shift in melting temperatures with increasing B_4C content is confirmed by temperature estimates based on the time of rapid transition from low to higher gas release rates as shown in Fig. 16. All Zr-bearing melts are oxidized

Table 1
Composition of absorber melts for oxidation tests.

Nos.	B_4C wt.%	SS wt.%	Zry wt.%
1	0	100	0
2	5	95	0
3	10	90	0
4	20	80	0
5	30	70	0
6	9	81	10
7	7	63	30
8	0	70	30
9	0	0	100
10	100	0	0

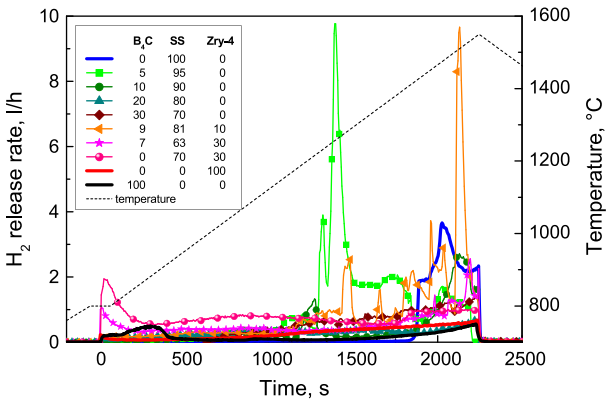

Fig. 16. Release of H_2 during transient oxidation of absorber melts in Ar/steam. Pure compounds are indicated by bold lines for comparison.

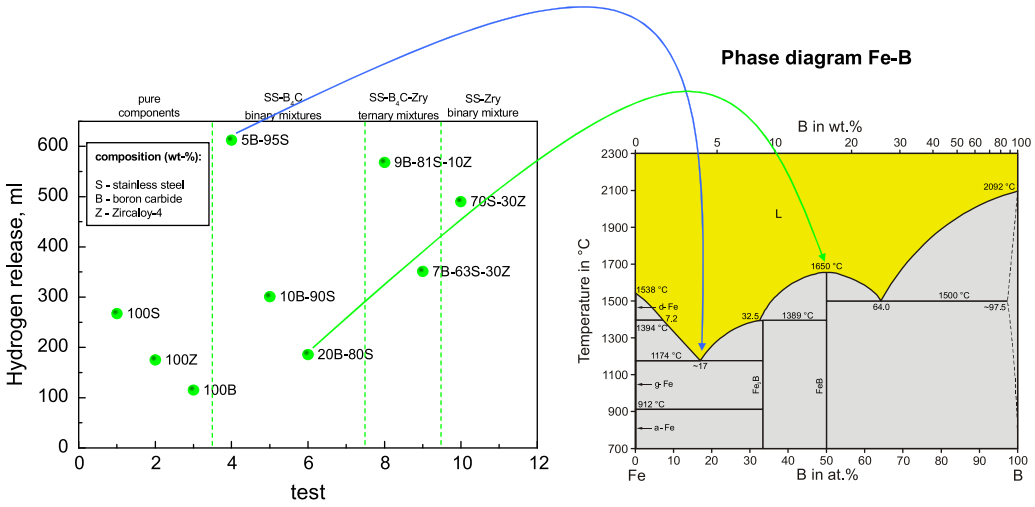

Fig. 17. Integral hydrogen release during oxidation of pseudo-binary and pseudo-ternary absorber melts as well as of the pure components during transient oxidation in steam (left) and Fe–B phase diagram (right).

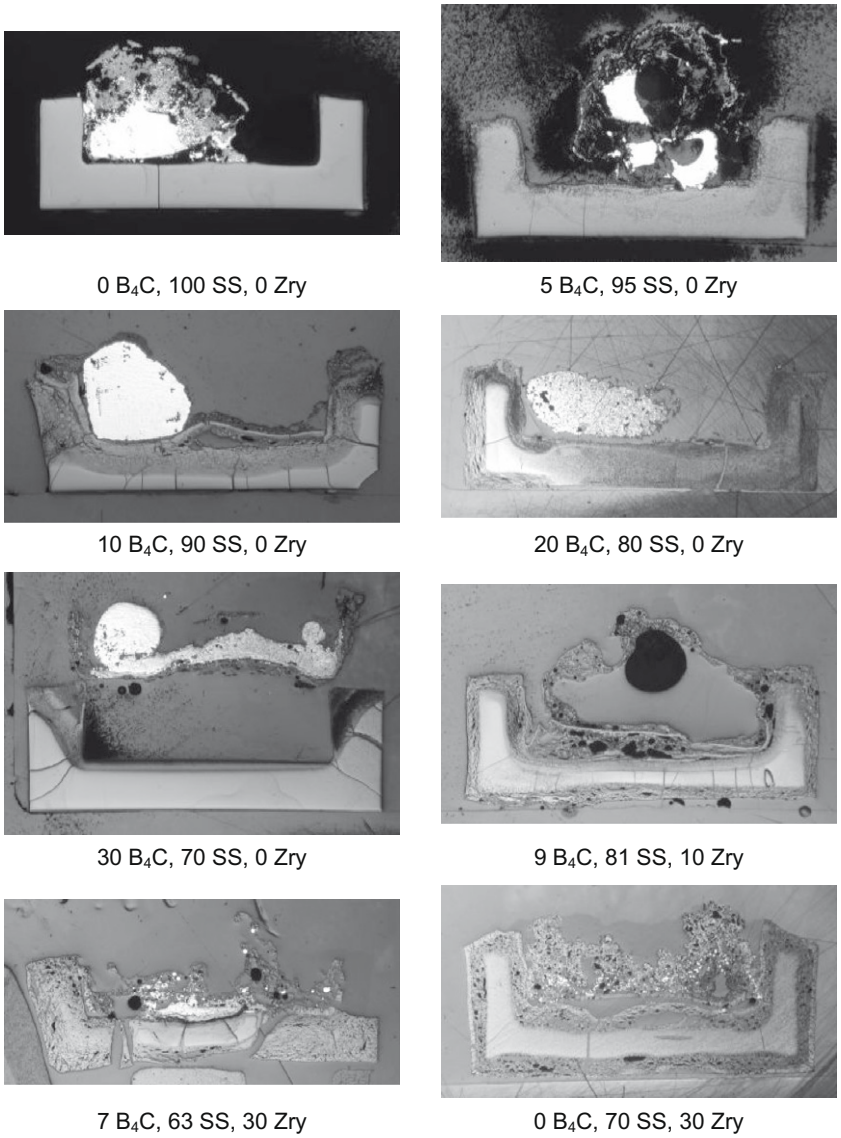

Fig. 18. Cross sections of absorber melt specimens before (left) and after (right) transient oxidation in steam at 800–1550 °C.

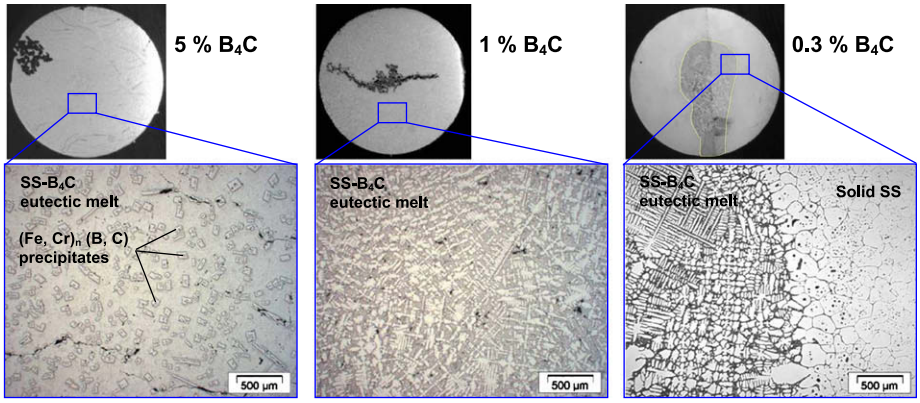

Fig. 19. SS/B_4C specimens with 5 wt.%, 1 wt.%, and 0.3 wt.% boron carbide after 1 h at 1250 °C in an inert atmosphere.

completely. They attacked the (Y_2O_3-stabilized) ZrO_2 crucibles most aggressively.

3.6. Tests of stainless steel liquefaction by boron carbide

It was demonstrated above that fast, complete liquefaction of the stainless steel absorber rod cladding takes place above some 1250 °C without complete or even considerable consumption of the boron carbide pellets. Hence, the question arose, how much steel can be liquefied by the eutectic interaction with B_4C approx. 200 K below its melting temperature.

Various tests were performed on stainless steel (AISI 304) hollow cylinder specimens with central boron carbide pellets in an inert atmosphere in the LAVA furnace. The specimens with different B_4C masses (5 wt.%, 1 wt.%, and 0.3 wt.%) were held at approx. 1250 °C for 1 h to allow equilibrium conditions to be established. Other tests involving shorter times at plateau temperature (300, 0 s) of medium-size B_4C pellets, and one reference test of a hollow cylinder of pure stainless steel were performed for comparison. The specimens with three different boron carbide cylinders kept in a zirconia crucible and covered with an yttria disc are shown in Fig. 2.

The boron carbide was consumed completely in the 1 h tests, as can be seen in Fig. 19. 5 wt.% and 1 wt.% boron carbide completely liquefied the stainless steel, whereas only 26% of the specimen with 0.3 wt.% B_4C was liquefied. (The black zones in the two overview images on the left are pores produced during cooling.) The enlarged metallographic images in Fig. 19 show homogeneous melt production for the specimens with higher B_4C contents and the transition between eutectic melt and still solid stainless steel for the specimen with the smallest B_4C pellet. Block shaped and needle-like precipitates of iron/chromium borides with some dissolved carbon $(Fe, Cr)_n(B, C)$, with n between 1.8 and 2.7, were found in the specimens with the highest B_4C content. The complex eutectic matrix mainly consists of boron-free (Fe, Cr, Ni) carbides and (Fe, Cr) carbides as well as borocarbides similar in composition to the large block crystals (but with higher carbon contents). The phase composition of the solidified eutectic melt of the 1 wt.% specimen also consists of boron-free (Fe, Cr, Ni) carbides and (Fe, Cr) borocarbides. As expected, a reference specimen of pure stainless steel exposed to the same temperature history did not show any evidence of molten phases.

Two more tests of 1 wt.% B_4C were performed with much shorter times at temperature. They confirmed liquefaction to take place very rapidly. After five minutes, the boron carbide pellet was almost consumed and roughly half of the steel sample was liquefied. Even after <1 min at a temperature above 1200 °C, a significant amount of steel was molten by the eutectic interaction with B_4C. These results are in agreement with Nagase et al. [4] who found strongly increased reaction kinetics between B_4C and SS in the temperature range 1200–1225 °C due to the formation of eutectic liquid phases.

4. Summary and conclusions

Extensive tests of the degradation of boron carbide control rods and oxidation of the resultant absorber melts were performed.

Eutectic interactions of stainless steel, zircaloy and boron carbide, respectively, rapidly produce complex melts at temperatures of approx. 1250 °C. These low-viscosity melts relocate downward inside the gap between the B_4C pellets and the external oxide scale developed on the guide tube surface, which prevents early oxidation and radial distribution of the melt. After failure of the oxide shell, oxidation of the absorber melt takes place very rapidly. Also, the pseudo-ternary SS/B_4C/Zry melt attacks the cladding (oxide scale) of the surrounding fuel rods in oxidizing atmosphere and may initiate early releases of fuel and fission products.

The behavior of a control rod of a French PWR design in dependence as a function of temperature can be summarized as follows:

1000 °C: no significant interactions of stainless steel, boron carbide, and Zircaloy.
1200 °C: local interactions of stainless steel, boron carbide, and Zircaloy (see [2,4,17], and [18] for kinetic data).
$\geqslant$1250 °C: rapid, complete liquefaction of metals (steel, Zircaloy) in the gap between B_4C pellet and external ZrO_2 oxide scale.
$\geqslant$1450 °C: failure of the oxide scale and rapid oxidation of absorber melt and remaining B_4C pellets.

Oxidation of the B_4C-bearing melts leads to the production of CO, CO_2, and boric acids and to a significant additional release of hydrogen. As for the oxidation of pure B_4C, no methane was released in these high-temperature oxidation tests. The melts oxidize much faster than solid materials at the same temperatures because of fragmentation and the development of non-protective oxide scales.

Finally, it was shown that boron carbide is able to liquefy large amounts of steel at 200 K below its melting temperature; a specimen with 99 wt.% steel and 1 wt.% B_4C was molten completely after 1 h at approx. 1250 °C, and significant amounts of steel were liquefied after a few minutes at temperature.

Although the number of control rods in a nuclear reactor is small in comparison with the number of fuel rods, their degradation and oxidation may influence integral bundle degradation during severe accident sequences. The production of melts at low

temperatures initiates local fuel rod failure associated with an early release of fission products. Moreover, oxidation of B_4C and melts containing B_4C is rapid and strongly exothermal, causing local releases of chemical energy in the bundle and possibly triggering more global temperature escalations. The influence of a boron carbide absorber rod on bundle degradation and behavior during reflooding was also demonstrated in the QUENCH-07 and QUENCH-09 bundle experiments [12,13].

Acknowledgments

The experiments described in this report were co-financed by the European Commission under the Euratom Fifth Framework Programme on Nuclear Fission Safety 1998–2002. Metallographic analyses of the specimens by U. Stegmaier, and extensive elemental analyses by Auger spectroscopy by E. Nold, as well as experimental support provided by A. Meier (all KIT/IMF-I), are gratefully acknowledged. Finally, the author wishes to thank Mr. Friese for the careful English review of this paper.

References

[1] Y. Kawada, Reactors and Materials of Nuclear Elements Containing Boron, Note Technique SEMAR 98/67, IPSN Cadarache, 1998 (May).
[2] P. Hofmann, M.E. Markiewicz, J.L. Spino, Nucl. Technol. 90 (1990) 226–244.
[3] L. Belovsky et al., Chemical interaction in B_4C-filled control rod segments above 1000 °C under transient conditions, in: 5th International Conference on Nuclear Engineering ICONE5, Paper 2148, Nice, France, May 26–29, 1997.
[4] F. Nagase, H. Uetsuka, T. Otomo, J. Nucl. Mater. 245 (1997) 52–59.
[5] M. Steinbrück, A. Meier, U. Stegmaier, L. Steinbock, Experiments on the oxidation of boron carbide at high temperatures, Report FZKA 6979, Forschungszentrum Karlsruhe, 2004.
[6] W. Krauss, G. Schanz, H. Steiner, TG-Rig tests (thermal balance) on the oxidation of B_4C, Basic Experiments, Modelling and Evaluation Approach, Report FZKA 6883, Forschungszentrum Karlsruhe, 2003.
[7] Dominguez, N. Cocuaud, D. Drouan, A. Constant, D. Jacquemain, J. Nucl. Mater. 374 (2008) 473–481.
[8] M. Steinbrück, J. Nucl. Mater. 336 (2005) 185–193.
[9] B. Adroguer et al., Nucl. Eng. Design 235 (2005) 173–198.
[10] G. Repetto et al., Prog. Nucl. Energy 52 (2010) 37–45.
[11] B. Clement, Main lessons learnt from the Phébus FP programme and follow-up, American Nuclear Society Spring Meeting, ANS Transactions, vol. 98, Anaheim, California, June 8–12, 2008.
[12] M. Steinbrück et al., Results of the B_4C Control Rod Test QU-07, Report FZKA 6746, Forschungszentrum Karlsruhe, 2004.
[13] M. Steinbrück et al., Results of the QUENCH-09 Experiment with B_4C Control Rod, Report FZKA 6829, Forschungszentrum Karlsruhe, 2004.
[14] P. March et al., in: International Conference on Nuclear Engineering (ICONE 14), First Results of the Phebus FPT3 Test, vol. 14, Miami, FL (United States), 17–20 July, 2006.
[15] M. Steinbrück, A. Meier, E. Nold, U. Stegmaier, Degradation and Oxidation of B_4C Control Rod Segments at High Temperatures, Report FZKA 6980, Forschungszentrum Karlsruhe, 2004.
[16] TAPP2.2: A Database of Thermochemical and Physical Properties, ES Microware, Hamilton, Ohio, 1994 (and references herein).
[17] M.S. Veshchunov, P. Hofmann, J. Nucl. Mater. 210 (1994) 11–20.
[18] M.S. Veshchunov, P. Hofmann, J. Nucl. Mater. 226 (1995) 72–91.